# SPINODAL LINES AND EQUATIONS OF STATE: A REVIEW

John H. LIENHARD, N. SHAMSUNDAR and Paul O. BINEY *

*Heat Transfer/Phase-Change Laboratory, Mechanical Engineering Department, University of Houston, Houston, TX 77004, USA*

The importance of knowing superheated liquid properties, and of locating the liquid spinodal line, is discussed. The measurement and prediction of the spinodal line, and the limits of isentropic pressure undershoot, are reviewed. Means are presented for formulating equations of state and fundamental equations to predict superheated liquid properties and spinodal limits. It is shown how the temperature dependence of surface tension can be used to verify $p-v-T$ equations of state, or how this dependence can be predicted if the equation of state is known.

## 1. Scope

Today's technology, with its emphasis on miniaturizing and intensifying thermal processes, steadily demands higher heat fluxes and poses greater dangers of sending liquids beyond their boiling points into the metastable, or superheated, state. This state poses the threat of serious thermohydraulic explosions. Yet we know little about its thermal properties, and cannot predict process behavior after a liquid becomes superheated. Some of the practical situations that require a knowledge the limits of liquid superheat, and the physical properties of superheated liquids, include:

- Thermohydraulic explosions as might occur in nuclear coolant line breaks, liquefied light-hydrocarbon spills, or Kraft paper process boiler leaks.
- Quenching, as occurs in heat treating metals, rewetting nuclear cores, cooling liquid metal ejecta from a melted reactor core, or the diagnosis of boiling heat transfer.
- Predicting the behavior of liquids heated beyond their boiling points, in nucleate and transition boiling.
- Estimating how much damage a thermohydraulic explosion can do.

Much of the work reviewed here was the result of previous inquiries supported by the Electric Power Research Institute. The results developed under EPRI support included: a fundamental equation for water in the superheated liquid and subcooled vapor states [1,2];

---

* Present address: Mechanical Engineering Department, Prairie View A&M University, Prairie View, TX 77446, USA

methods for making simplified predictions of property information, which can be applied to the full range of fluids – water, mercury, nitrogen, etc. [3–5]; and predictions of the depressurizations that might occur in thermohydraulic accidents. (See e.g. refs. [6,7].)

## 2. The spinodal limit of liquid superheat

### 2.1. The role of the equation of state in defining the spinodal line

Fig. 1 clarifies what happens when a liquid is heated beyond its boiling point. It shows real isotherms of a fluid on $p-v$ coordinates. All states along an isotherm are *equilibrium* states. When the slope of an isotherm is positive, that equilibrium is *unstable*. When the slope is negative, the equilibrium is *stable*. The *spinodal* line connects the points where the isotherms have zero slope. By locating the liquid spinodal line, one specifies the absolute limit beyond which a liquid can never be superheated. Another feature of this curve is that the Gibbs potentials, $g_f$ and $g_g$, must be equal in the saturated liquid and vapor states. Thus:

$$g_g - g_f = 0 = \int_f^g (v \, dp - s \, dT)_T. \tag{1}$$

The last term vanishes giving the "Gibbs–Maxwell" relation, which requires that area A in fig. 1 equals area B:
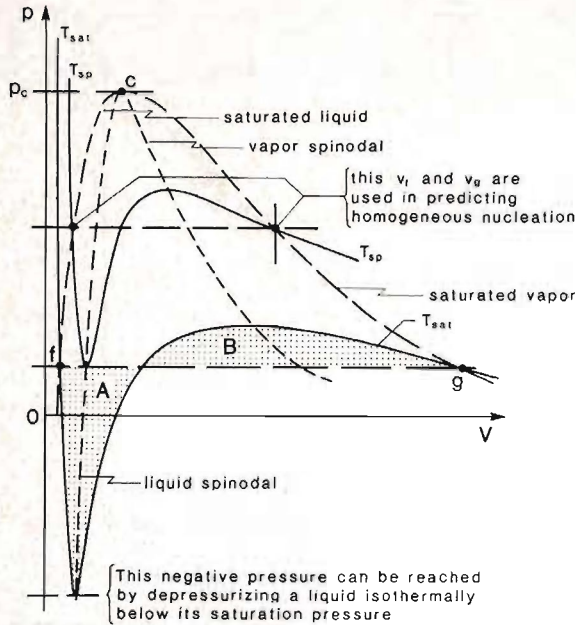
$$\int_f^g v \, dp = 0. \tag{2}$$

Fig. 1. Typical real-gas isotherms.

For a long time, van der Waals' equation

$$p = \frac{RT}{v-b} - \frac{a}{v^2}, \tag{3}$$

provided the only theoretical knowledge of real fluid isotherms. Van der Waals argued, on the basis of molecular behavior, that there is an inherent continuity from the liquid to the vapor states. An important feature of this equation is that it can be nondimensionalized using critical data. Thus:

$$p_r = \frac{8T_r}{3v_r - 1} - \frac{3}{v_r^2}, \tag{4}$$

where $p_r = p/p_c$, etc. The dimensionless van der Waals equation suggests the Law of Corresponding States – that one equation of state, written in reduced coordinates, should describe all fluids.

Today, we know that the Law of Corresponding States should be written as:

$$p_r = f(T_r, v_r, \text{ primary molecular parameter, other}$$

$$\text{molecular parameters}) \tag{5}$$

– The strongest influences in eq. (5) are those of $T_r$ and $v_r$. Indeed the need for any further parameters was not clarified until the mid 1950's.

– The primary molecular parameter is usually taken to be $Z_c$; the Riedel factor, $\alpha_p$ (see ref. [8]); or the Pitzer acentric factor, $\omega$ (see, e.g. ref. [9]):

$$\omega \equiv -1 - \log_{10}[p_{r,sat}(T_r = 0.7)].$$

Fig. 2 is a recent Corresponding States correlation [5] of the ratio $v_f/v_g$. The use of the Pitzer factor here brings data for very different fluids into alignment.

– Little has been done with secondary molecular parameters. Fig. 3 shows how data for molecules with high dipole moments deviate slightly from an otherwise successful correlation of burnout heat fluxes, based on the Law of Corresponding States [10]. Thus the Law sometimes needs correction when it is applied to polar molecules.

An interesting corollary to the preceding results is that van der Waals' equation should accurately describe any real fluid with $Z_c$, $\alpha_R$, or $\omega$ equal to the van der Waals' value. We therefore ask if there is any such fluid.

Fig. 4 shows the raw data that established fig. 2. When they are cross-plotted against $\omega$ (in the inset), all, *including the van der Waals value*, lie on the same straight line. Furthermore, $v_f/v_g$ for mercury ($\omega = -0.21$) closely approximates that of the van der Waals fluid whose $\omega$ of $-0.302$ is only slightly lower.

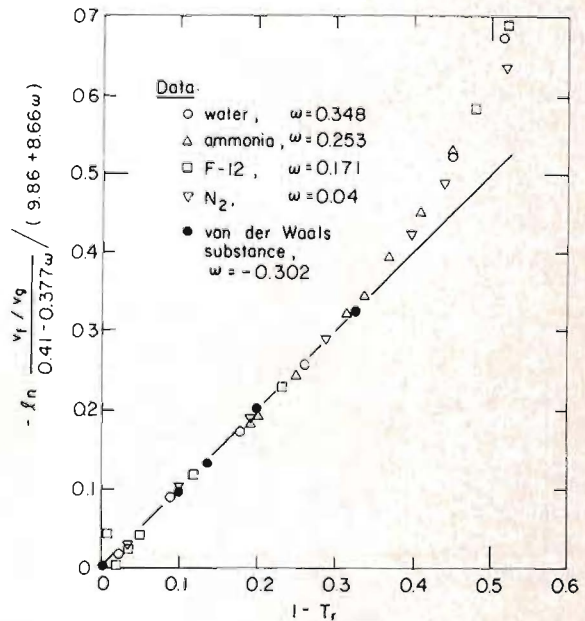The importance of this is that – since van der Waals'



Fig. 2. The use of the Pitzer factor to complete a Corresponding States correlation of $v_f/v_g$ (from ref. [5]).
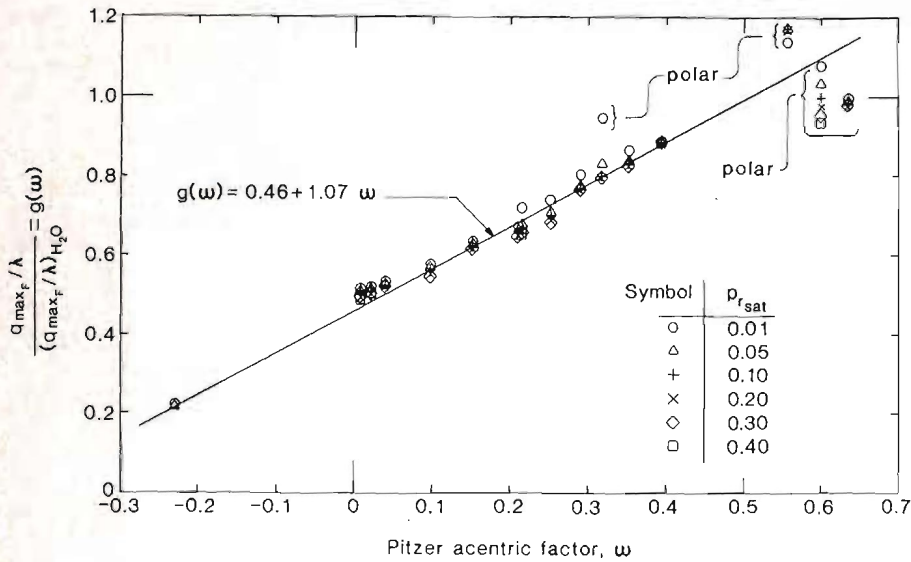
Fig. 3. Illustration of the failure of polar fluids to conform to a Corresponding States correlation (from ref. [10]).

equation yields a pair of spinodal lines and it is the basis for the Law of Corresponding States – real-fluid spinodal lines should also obey the Law of Corresponding states.
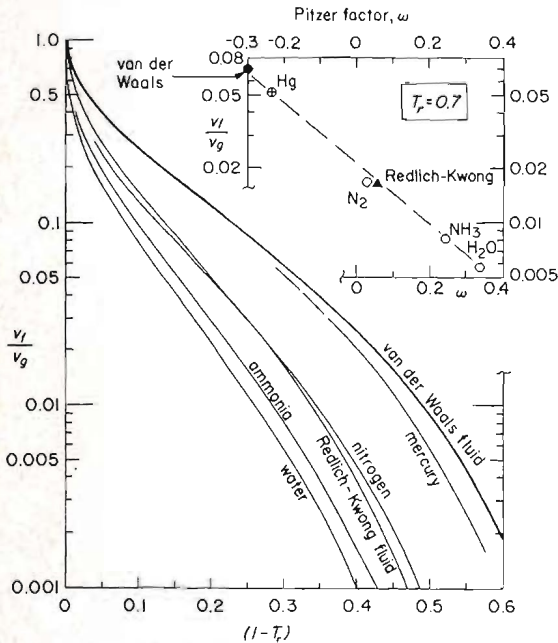


Fig. 4. Construction of the correlation in fig. 2 illustrating the influence of the Pitzer factor.

The van der Waals spinodal lines are obtained by setting $(\partial p_r / \partial v_r)_T = 0$ and eliminating $T_r$ between this result and the original equation. The result:

$$p_r = 3/v_r^2 - 2/v_r^3,$$
(6)

describes the liquid spinodal for $v_r < 1$ and the vapor spinodal for $v_r > 1$.

### 2.2. Relation of the spinodal line to the homogeneous nucleation limit

We would like to use measurements of the limiting liquid superheat to obtain the location of the spinodal line. But can that be done? Are the homogeneous nucleation limit and the spinodal line related? To bring a real liquid all the way up to the spinodal limit, one would have to do so without *any* disturbances or imperfections in the system. However, real liquids are made of molecules that constantly move. As the liquid temperature rises these motions provide the disturbances needed to upset liquid stability at a temperature *less* than the spinodal temperature.

Frenkel (see e.g. ref. [11]) first calculated the least disturbance needed to create a minimum stable vapor bubble or the "potential barrier" to nucleation. He calculated the difference in Gibbs function of the liquid with and without an unstable vapor bubble in it and obtained the critical work, $Wk_{crit}$, needed to create the

bubble:

$$Wk_{crit} = \tfrac{4}{3}\pi R_0^2 \sigma. \tag{7}$$

The radius, $R_0$, is the well-known unstable equilibrium radius:

$$R_0 = \frac{2\sigma}{p_{sat\ at\ T_{sup}} - p}, \tag{8}$$

where $T_{sup}$ is the local temperature of the superheated liquid, and $p$ is the pressure in the surrounding liquid.

$Wk_{crit}$ must now be compared with a characteristic energy of the superheated liquid. Two energies are appropriate to this purpose:

- The average level of molecular vibrational energy is on the order of $kT$, where $k$ is Boltzmann's constant and $T$ is $T_{sup}$ – the temperature of the superheated liquid. Conventional theories of homogeneous nucleation are based on this energy.
- The energy required to separate two molecules from one another. This is the depth of the "potential well" and it is well known to be on the order of $kT_c$. The use of $kT_c$ was introduced in ref. [3], and is discussed below.

The ratio of $Wk_{crit}$ to $kT$ (or $kT_c$) is the Gibbs number:

$$Gb \equiv Wk_{crit}/kT. \tag{9}$$

What is the minimum Gb for which nucleation absolutely must occur? The least possible value of $R_0$ will give the minimum $Wk_{crit}$ and Gb. To find it, we first define:

$j \equiv$ probability of nucleating a bubble

in a given molecular collision. $\qquad$ (10)

Now $j$ must be 1 for $Gb = 0$, and we expect that:

$$\frac{dj}{j} = -\frac{dWk_{crit}}{kT\ or\ kT_c} = -dGb, \tag{11}$$

so:

$$j\frac{nucleation\ events}{molecule\ collisions} = e^{-Gb}. \tag{12}$$

The problem thus reduces to establishing $j$. To do this, consider a spherical region of undisturbed liquid in which the smallest critical bubble, with radius $R_0$, might nucleate, and then count the rate at which collisions can occur in this region (fig. 5). Nucleation must occur if just one of these collisions triggers a critical nucleus within one relaxation time (or about 10 collisions). This gives:

Probability of nucleation $= j \leq 10^{-5}$.
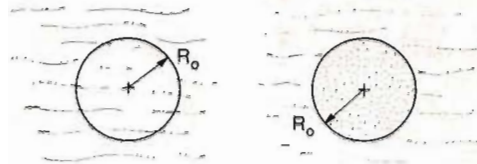


Liquid in which a bubble of radius $R_0$ will form.

An unstable bubble nucleus displaces N liquid molecules, each of which suffers about $10^{13}$ collisions per sec.

Fig. 5. Model for calculating the maximum $j$.

It was thus shown in ref. [3] that the limiting value of $j$ is $10^{-5}$. This limit, of course, is only an order of magnitude estimate. Fortunately, nucleation is only sensitive to large variations in $j$. (Later we suggest $2 \times 10^{-5}$ might be a better value.)

We now have a prediction for the limit of homogeneous nucleation. To find how close to the the spinodal line it lies, we use the thermodynamic availability of spinodal liquid, with respect to liquid at the limit of homogeneous nucleation:

$$\Delta a|_{h.n.}^{sp} = Gb_{min}(kT\ or\ kT_c), \tag{13}$$

where $Gb_{min} = -\ln(2 \times 10^{-5}) = 10.8$, and the isobaric difference in availabilities is:

$$\Delta a|_{h.n.}^{sp} = [\Delta h - T_{h.n.}\Delta s]_{h.n.}^{sp}. \tag{14}$$

It is shown in ref. [3] that eq. (14) implies a $\Delta T$ on the order of $1°C$ between the homogeneous nucleation and spinodal lines. Therefore the *liquid* spinodal line can be located with high accuracy using a homogeneous nucleation prediction. We make this prediction by combining eqs. (7) and (8) in eq. (12). The final result, which includes a curvature correction (see ref. [11]), $(1 - v_f/v_g)^2$ that cannot be obtained from eq. (7), (8) and (12), is:

$$10.8 = \frac{16\pi\sigma^3}{3(kT)\left[p_{sat}(T_{sp}) - p\right]^2(1 - v_f/v_g)^2}. \tag{15}$$

The terms $T_{sp}$, $v_f$, and $v_g$ are defined in fig. 1. The term $kT$ is $kT_{sp}$ in the conventional theory, but we show in section 3 that it probably should be $kT_c$.

When this argument is applied to the nucleation of liquid drops in a vapor – which is less dense – far fewer nucleation events are needed in the limiting case of complete nucleation. Thus, $j$ must be far smaller and

Gb far larger. This leads to large temperature differences between homogeneous nucleation and the vapor spinodal.

## 2.3. Experimental data for homogeneous nucleation at high superheat, or large values of j

V. Skripov and his coworkers at the Ural Institute at Sverdlovsk have pushed the limit of liquid superheat much further in the laboratory than anyone else. Much of this work is summarized in two books [11,12]. Avedisian [13] recently provided an extensive compendium of measured liquid superheat and related $j$ values *.

Many techniques exist for creating high liquid superheats. The most effective has been Skripov's method of pulse heating a fine wire filament. When the wire is subjected to a known electrical pulse, its temperature rises rapidly and predictably within a few microseconds. As the temperature rises, a few isolated instances of nucleation occur; but then – at a certain temperature – a complete blanket of vapor appears on the wire. It is at this point that no further temperature increase is possible in the liquid.

Skripov reached different limiting temperatures depending upon the rate at which he heated the liquid. However, as the heating rate rose, the temperature approached an asymptote. The value of $j$ at that limit was about $10^{-5}$. (Skripov reports some values of $j$ slightly above $10^{-5}$, but only at heating rates for which a different and less reliable experimental technique was used.)

Fig. 6 shows those data of Skripov et al., available in 1976 [14], for $j$ values on the order of $10^{-13}$. The difference between his homogeneous nucleation temperature and the saturation temperature at the same pressure, is plotted against $T_r$. The notational distinction between fsp (liquid spinodal) and gsp (vapor spinodal) is introduced temporarily in fig. 6 because it includes the best data available for nucleation of droplets in subcooled vapor. The liquid and vapor spinodal limits calculated from van der Waals' equations are also included.

Fig. 6 makes two things clear: One is that the homogeneous nucleation limits for the 12 liquids do conform to Corresponding States correlation. Furthermore, the shape of the dashed correlating line through them is very similar in form and placement to the van der Waals prediction. This corroborates the demonstra-

tion [3] that these data should be almost the same as the spinodal line which is a *thermodynamic* variable. The second point made clear in fig. 6 is that – as we anticipated – the vapor nucleation data do not in any way conform to Corresponding States correlation.

In ref. [14] the following equation was fitted to the Skripov data:

$$\Delta T_r = 0.905 - T_{r,\text{sat}} + 0.095\, T_{r,\text{sat}}^8. \tag{16}$$

This gives values slightly less than the true generalized spinodal value, because $j$ for this set of Skripov's data is a factor of $10^{-8}$ smaller than the spinodal $j$ *.

All the variables in eq. (15) are subject to corresponding states correlation. Forming such a correlation for the limit of pressure undershoot was the subject of ref. [5]. This result, based on $kT_c$ instead of $kT$, was:

$$\Delta p_r = p_{\text{sp}} - p_{\text{sat}}$$
$$= \frac{112.82 + 224.42\,\omega}{\sqrt{-\ln(j)}} \left(1 - T_{r,\text{sp}}\right)^{1.83}. \tag{17}$$

See fig. 1 for notation and note that, while $j \approx 2 \times 10^{-5}$ gives the spinodal line, any smaller $j$ gives a homogeneous nucleation limit that does not reach the spinodal line.

The Corresponding States correlation can also be written in terms of temperature. The result for the spinodal line can be approximated with high accuracy in the form:

$$\Delta T_r = 0.923 - T_{r,\text{sat}} + 0.077\, T_{r,\text{sat}}^9. \tag{18}$$

This lies about 2% above the correlation given by eq. (16), and reflects the increase of $j$ from the value of $10^{-13}$ (which was characteristic of Skripov's experiments) to $2 \times 10^{-5}$.

## 3. The development of equations of state and fundamental equations to describe the metastable regions

We can now place the spinodal limit with reasonable accuracy. However thermodynamic properties are generally unavailable in the metastable and unstable ranges. Such data are constantly needed in boiling and two-phase heat transfer work, but they are extremely hard to come by, and little analysis has been done.

It has been customary in boiling work to estimate

---

* Actually, Skripov (and Avedisian as well) use $J$ instead of $j$. $J$ is equal to $j$ multiplied by the rate of molecular collisions per cm$^3$. $J$ is normally about $10^{39}$ times $j$ in these units.

* People unfamiliar with these calculations will understandably be startled at the notion that a factor of $10^{-8}$ makes so little difference in this range.
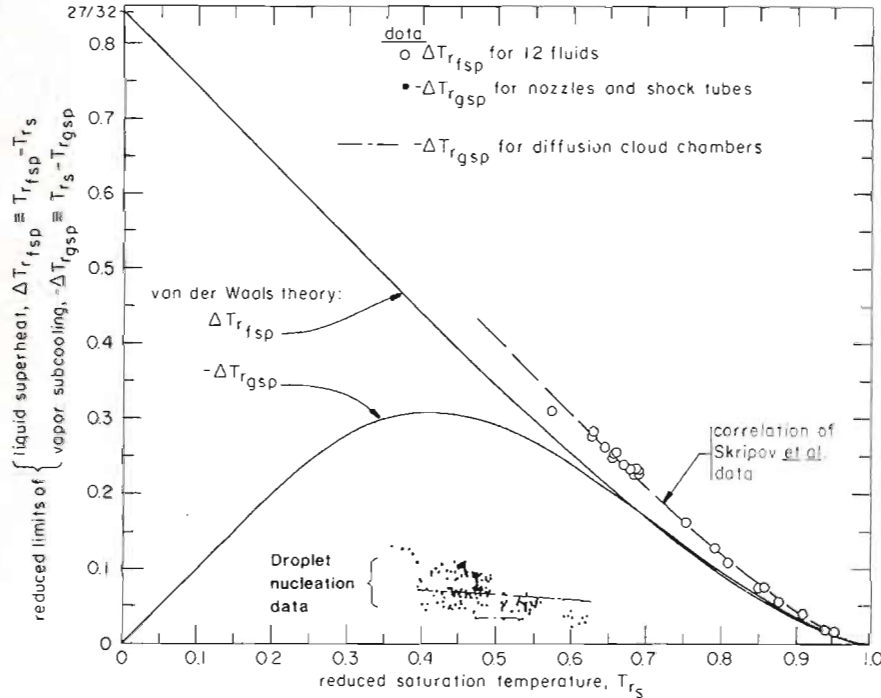
Fig. 6. Corresponding States correlations of the limiting liquid superheat and vapor subcooling.

thermodynamic properties in these regimes by extrapolating them linearly in temperature. This works in slightly superheated liquids, but at higher superheats such a simple strategy becomes impossible. (The specific heat at constant pressure approaches infinity on spinodal lines, liquids become highly compressible at high superheat, etc.)

### 3.1. The formulation of fundamental equations

The "fundamental" or "canonical" thermodynamic equation is one from which all equations of state can be derived and in which all thermodynamic properties are embodied. Four common ones for a pure substance take the forms $s = s(u, v)$, $h = f(s, p)$, $\psi = \psi(T, v)$ and $g = g(T, p)$. The several equations of state are obtained from the derivatives of these equations with respect to their independent variables. For example, the $p$–$v$–$T$ and energy equations of state are obtained from:

$$p/T = (\partial s/\partial v)_u \quad \text{and} \quad 1/T = (\partial s/\partial u)_v. \tag{19}$$

One tends to associate the $p$–$v$–$T$ equation with the term "equation of state"; but it gives incomplete thermodynamic information and must be combined with a "caloric", or specific heat, equation of state to give – say – enthalpies or entropies. A *fundamental equation*, when it can be written, is more convenient than a set of equations of state. It provides all thermodynamic information through straightforward calculations. The Helmholtz function form of the fundamental equation, for example, can be obtained from the $p$–$v$–$T$ and $c_p^0$ equations:

$$\psi(v, T) = \psi_{ref} + \int_v^{RT/p_{ref}} p \ dv'$$
$$+ \int_{T_{ref}}^T c_p^0(T')[T/T' - 1] \ dT'$$
$$- R(T - T_{ref}), \tag{20}$$

where $(p_{ref}, T_{ref})$ is a reference point where the ideal gas equation is valid and the entropy is taken as zero.

The Steam Tables (see, e.g., ref. [15] or ref. [16]) are normally based on empirical fundamental equations in the Helmholtz form with scores of constants in them. Such equations permit one to evaluate any thermodynamic property within four decimal places. But we seldom have anything nearing such complete property information for fluids other than water. Furthermore,

such equations do not normally provide valid information in the metastable regimes.

### 3.2. Surface tension

The property, surface tension, $\sigma$, is important in predicting the burnout heat flux – a crucial design variable in any energy system in which heat is removed by boiling. Unfortunately, it has not been measured over wide ranges of temperature for many fluids.

Furthermore, $\sigma$ is intimately related to the $p-v-T$ equation of state. Van der Waals – well known for his remarkably simple and successful equation of state – also developed this remarkable and completely precise equation for predicting the surface tension, $\sigma$, from a knowledge of the $p-v-T$ equation of state [17]:

$$\sigma = \sigma_0 \int_{v_{r_f}}^{v_{r_g}} \frac{1}{v_r^{5/2}} \left[ p_{r,\text{sat}}(v_r - v_{r,f}) \right.$$

$$\left. - \int_{v_{r_f}}^{v_r} p_r \, dv_r \right]^{1/2} dv_r. \tag{21}$$

The integration of eq. (21) requires complete $p-v-T$ values in the metastable and unstable regimes. Thus surface tension can be used to extend metastable property information and vice versa.

### 3.3. Karimi's fundamental equation for water

Karimi made the first attempt to create an accurate fundamental equation for water in the metastable regimes. He and Lienhard first [1] made a relatively crude modification of the Keenan–Keyes–Hill–Moore (KKHM) equation of state for water [15]. Karimi then refined the curve-fit and produced a greatly improved equation [2].

Some of the important results predicted by Karimi's equation are shown in the modified $p-v-T$ and $T-s-p$ surfaces shown in figs. 7 and 8. Notice that all of the properties exhibit continuous change as they pass into the "two-phase" regime. The stable, metastable, and unstable regimes are all shown, and the conventional straight-line representations of mixtures are not included.

Although Karimi's results point out the potential for accurately predicting metastable and unstable behavior of real substances, he had to use different coefficients on either side of $T = 150°C$ in his final equation. Consequently the equation displayed inconsistencies and discontinuities in the neighborhood of $150°C$.

Karimi based his work on the KKHM equation,

$$p = \rho RT \left[ 1 + \rho \frac{\partial}{\partial \rho}(\rho Q) \right] \tag{22}$$

where $Q$ is a function of $\rho$ and $T$, obtained by fitting the data to a suitable expression with many terms of the type $(T - a)^m (\rho - b)^n e^{-c\rho}$. KKHM only used data from the stable regions in their fitting. Karimi improved the coefficients with the help of additional theoretical constraints and the meager existing data for metastable fluids.

The KKHM equation is the sum of an ideal gas expression and a correction. No such features as changes of phase, stable and metastable regions, etc., can be modelled by this ideal gas "reference function". Many of Karimi's difficulties arose because he had to absorb all of the complexity of water in the correction term, $Q$.

### 3.4. An improved strategy for creating a fundamental equation

A new and highly accurate equation of state was developed at the National Bureau of Standards (NBS) by Haar, Gallagher, and Kell in 1979 [18]. It, too, gives pressure as the sum of a reference function and a residual correction, but the reference function has a theoretical basis. It displays all real fluid features qualitatively, and yields errors less than 1% in wide ranges of $T$ and $p$. Thus, its residual correction is much smaller than in the KKHM equation. It must only improve the accuracy – it need not provide all the features of real fluid behavior by itself. Thus it can be fitted accurately with fewer terms.

We are currently modifying the NBS equation in much the same way as Karimi modified the older KKHM equation. A key factor to doing this is the use of cubic equations to extrapolate $p-v-T$ data. We turn to this matter next.

### 3.5. Cubic equations of state

Cubic equations of state, of which the van der Waals equation is the prototype, have the smallest number of free parameters that can represent real data accurately. They are therefore much safer to use in estimating data than more complicated ones. They display major features of physical behavior correctly in relatively large interpolations, with no need for smoothing. When such equations have enough inherent flexibility and are carefully fitted, they are remarkably accurate at a very low cost of calculation.
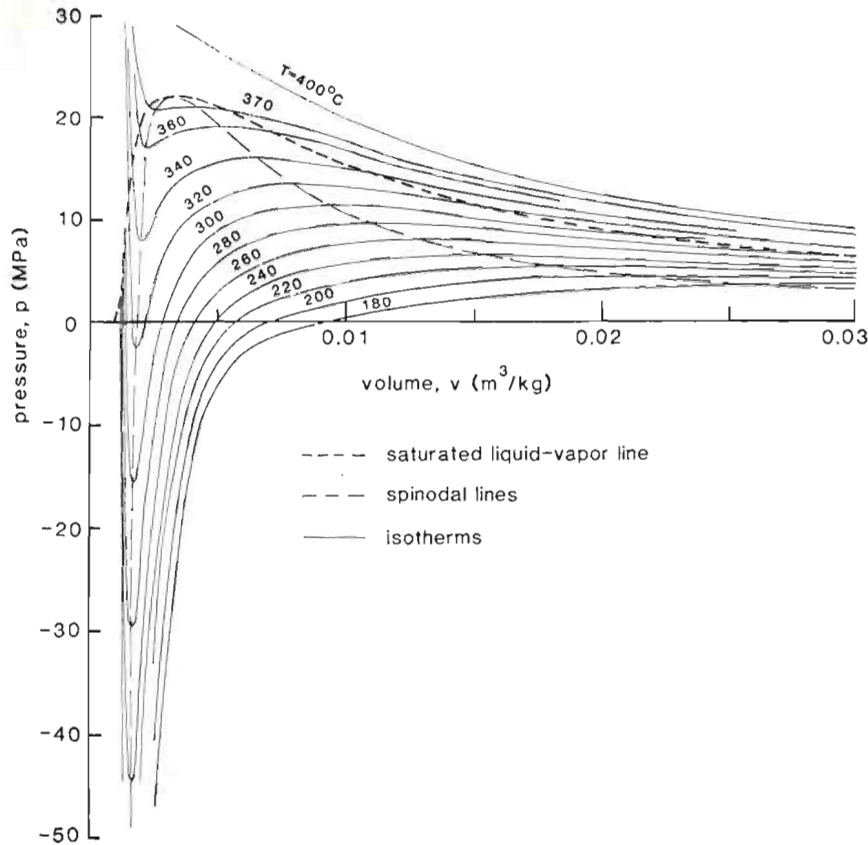
Fig. 7. The $p-v-T$ surface for water based on Karimi's [2] fundamental equation.

### 3.5.1. A new form of cubic equation

We have developed a new volume-cubic equation of state that includes most existing cubic equations of state as particular cases. General cubic equations have been developed by others, but their applicability has usually been restricted by tying some coefficients to certain groups of substances.

We avoid this trap by making the procedure for determining the coefficients as flexible as possible. When data are plentiful they can be used to fit the coefficients statistically, and the resulting equation will be very accurate. This can also be done with less accuracy when the data are less plentiful; but then the result can be used to back out unknown data – even critical data. A major strength of this equation is that it can be written in many forms – suiting the form to the number of data to be used in determining its coefficients.

The first form is of the same type as most existing cubic equations, with the coefficients normally – but not always – fitted with the help of critical data:

$$p_r = \frac{T_r}{r + b} - \frac{a T_r^{-\lambda}}{(r + c)^2 - d^2},$$
(23)

where $r \equiv (v_r - 1)Z_c$ and $b \equiv 1/\alpha$, and – if one elects to use the critical data – $a$, $c$, and $d$ become:
$a = (1 - b)^3$, $c = (1 - b)/2$, and $d^2 = c^2(1 - 4b)$. $\alpha$ is related to the Riedel factor, $\alpha_R$, by:

$$\alpha_R = \frac{\mathrm{d} p_{r,sat}}{\mathrm{d} T_r}\bigg|_{T_r=1} = \alpha(1 + \lambda) - \lambda.$$
(24)

The new variable, $r$, greatly simplifies the relations among the coefficients. It has the virtue of vanishing at the critical point, which is the natural origin for equations of state.

Eq. (23) includes many other familiar cubic equations as special cases. With $Z_c = \frac{3}{8}$, $\alpha = 4$ and $\lambda = 0$, we
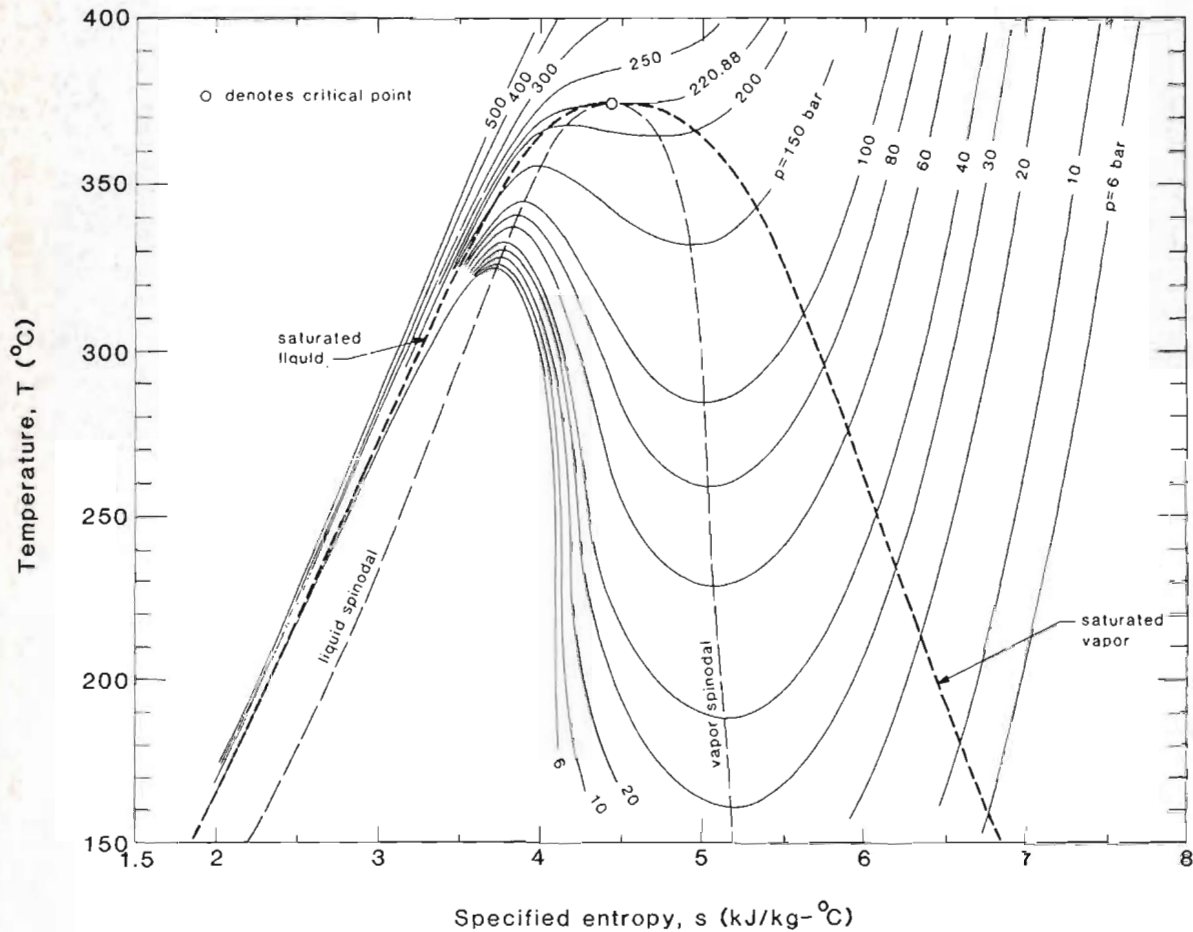
Fig. 8. The $T-s-p$ surface for water based on Karimi's [2] fundamental equation.

get the van der Waals equation; with $Z_c = \frac{1}{3}$, $\alpha = 3/(2 - 2^{1/3}))$ and $\lambda = \frac{1}{2}$ we get the Redlich–Kwong equation; etc.

We have yet to say how to assign a value to the coefficient $\lambda$. Often, $\lambda$ is chosen so as to make the equation better fit data away from the critical point, once the other constants have been fitted. However it might be unwise to rely this heavily on the critical point, which is mathematically singular as well as being a lone point. Indeed we have found that if, after using critical data for all but two constants, we fix both $\lambda$ and $\alpha_R$ using data away from the critical point, then $\alpha_R$ is liable to disagree with the measured value. This suggests that using data from all over the $p-v-T$ field might yield a better all-around equation if the critical point is allowed to float. We next see how this works.

### 3.5.2. Application of the cubic equation to a substance with a well-documented critical point

Water is extremely well-documented and existing cubic equations have generally failed to represent it at all well – particularly in the liquid state. We used $p_c$, $T_c$, and $v_c$ from the IFC 1967 Formulation [16], but not the published values of $\alpha_R$. Thus $b$ and $\lambda$ were unknowns obtained by fitting the equation to saturation data from the IFC skeleton table. Details of the fit are given in ref. [19]. The results – with very modest prediction errors – are reported in table 1. Saturated liquid properties are better represented by the present cubic equation than by any other, it predicts superheated vapor data very well, and it only shows inaccuracies in the compressed liquid range [19].

Table 1
Comparison of predictions from eq. (23) with IFC 1967 [16] data for water

| $T$ (°F) | $p_{sat}$ (psia) | $\delta p_{sat}$ (%) | $v_f$ (ft³/lb) | $\delta v_f$ (%) | $v_g$ (ft³/lb) | $\delta v_g$ (%) | $h_{fg}$ (Btu/lb) | $\delta h_{fg}$ (%) | |
|---|---|---|---|---|---|---|---|---|---|
| 198 | 9.783 | −3.9 | 0.01716 | −3.6 | 39.595 | 3.3 | 988.8 | 0.4 | |
| 250 | 30.41 | −2.8 | 0.01733 | −1.9 | 13.357 | 1.2 | 943.9 | 0.2 | |
| 286 | 54.47 | −0.7 | 0.01753 | −1.2 | 7.9282 | −0.2 | 917.3 | 0.3 | * |
| 370 | 171.7 | 1.0 | 0.01810 | 0.7 | 2.6842 | −2.3 | 849.7 | 0.4 | |
| 436 | 335.2 | 2.6 | 0.01878 | 2.2 | 1.3181 | −4.0 | 787.7 | 0.3 | * |
| 498 | 682.7 | 3.8 | 0.01954 | 3.3 | 0.7721 | −4.0 | 727.0 | 0.0 | |
| 536 | 899.8 | 3.5 | 0.02848 | 4.1 | 0.5889 | −3.8 | 665.1 | −0.2 | * |
| 586 | 1343 | 3.3 | 0.02203 | 4.4 | 0.3117 | −2.3 | 579.9 | −0.3 | * |
| 636 | 1955 | 2.4 | 0.02483 | 3.2 | 0.1859 | 1.1 | 461.5 | 8.9 | * |
| 678 | 2491 | 1.6 | 0.02879 | −8.5 | 0.1230 | 3.6 | 34109 | 3.4 | |
| 686 | 2798 | 0.8 | 0.03238 | −2.6 | 0.0949 | 6.4 | 256.7 | 8.2 | * |
| 698 | 2879 | 0.6 | 0.03371 | −3.5 | 0.0879 | 9.9 | 229.6 | 10.3 | |

* Data on these lines were not used in fitting the cubic.

### 3.5.3. Application of the cubic equation to substances with unknown critical data

When critical data are unknown, it is pointless to use eq. (23), whose volume variable, $r$, is centered on the critical point. One may then return to eq. (23) in its dimensional form and use non-critical data to determine the constants:

$$p = \frac{RT}{v - b} - \frac{a'T^{-\lambda}}{\left(v + c'\right)^2 - d'^2}.$$ (23a)

This was done for methane and water in ref. [19] with equal success. Table 2, for example, shows the results for methane. It is clear that such prediction is extremely accurate.

The liquid metals are natural substances for this application since, in most cases, tabulated data only go to a fraction of $T_c$. When the extrapolation is applied to mercury [20] and sodium [21], the results (table 2) are astonishing both in their accuracy and their implication. The critical point predictions for everything but $v_{c,sodium}$

(about twice the measured value) agree remarkably well with the published data. Consider what this implies:

The published $Z_c$ for mercury is close to the van der Waals value of $\frac{3}{8}$ and the calculated value is closer still. (We [4] recently presented other close agreements between the properties of mercury and the van der Waals fluid.) Thus mercury is very nearly a van der Waals fluid, and its reported critical data are probably accurate.

The predicted $T_c$ and $p_c$ for sodium are very nearly the same as the published values, so we are inclined to think these properties are known correctly. The measurement of $v_c$ is very difficult and often inaccurate. The value of $Z_c = 0.178$, based upon the reported $v_c$, is much lower than for other fluids. However, our prediction – $Z_c = 0.307$ – places sodium squarely among the light elements. It is thus likely that our $v_c$ and $Z_c$ values are the more correct ones, and that *the frequent suggestion that liquid metals are not subject to the Law of Corresponding States, is wrong.*

Table 2
Extrapolated critical constants obtained from eq. (23)

| Substance | Source | $p_c$(MPa) | $T_c$(K) | $v_c$(m³/kg) | $Z_c$ |
|---|---|---|---|---|---|
| Methane | Pred. | 4.600 | 190.52 | 0.006225 | 0.2914 |
|  | Litr. | 4.599 | 190.55 | 0.006233 | 0.2903 |
| Mercury | Pred. | 152.9 | 1870 | 0.0001913 | 0.377 |
|  | Litr. | 153.0 | 1763 | 0.0001818 | 0.381 |
| Sodium | Pred. | 34.09 | 2581 | 0.008411 | 0.307 |
|  | Litr. | 34.10 | 2573 | 0.004850 | 0.178 |

### 3.5.4. A second and very general form of cubic equation

If one or more of the constants in eq. (23) is allowed to vary with temperature its accuracy might be further improved. The obvious way to identify accurate forms of temperature dependence is to fit the equation at several temperatures, and then to form the functions by correlating the resulting coefficients with temperature.

To this end we turn to a second and far more general form of cubic equation that includes eq. (23) as a special case:

$$\frac{p}{p_{\text{sat}}} = 1 - \frac{(v - v_{\text{f}})(v - v_{\text{m}})(v - v_{\text{g}})}{(v + b)(v + c)(v + d)}. \tag{25}$$

The quantities $p_{\text{sat}}$, $v_{\text{f}}$, $v_{\text{m}}$, $v_{\text{g}}$, $b$, $c$ and $d$ all vary with temperature. The advantage of this form is that it automatically satisfies critical point criteria, but it need not be tied to them. Another nice feature is that it is prefactored to do away with the need for finding roots of the cubic in fitting the constants.

Three of the coefficients in eq. (25) are the known temperature-dependent properties: $p_{\text{sat}}$, $v_{\text{f}}$ and $v_{\text{g}}$. Thus the most straightforward use of the equation is one in which isotherms are fitted one at a time.

Actually, two of these constants can be fixed with the ideal gas law limit at low pressure and the Gibbs–Maxwell equal-areas condition (eq. (2).) Then just two pieces of data will fit an equation that should be quite accurate along a given isotherm.

The isothermal compressibility of saturated liquid, and one compressed liquid point, have proven to give the best results. It turns out that if the two missing pieces of data are reduced to just one by the seemingly arbitrary assumption that $c = d$, the resulting equation is still very accurate. For a given temperature, the coefficients for the equation can be found using very few data, and making a direct, not a statistical, calculation.

The remaining problem associated with this kind of use of eq. (25) – that of generalizing the temperature dependence of the coefficients – remains to be solved.

### 3.5.5. Applications of the cubic equation with temperature-dependent coefficients

The temperature-by-temperature application of eq. (25) to water has yielded accuracies that are *within the tolerance* of the IFC [16] Skeleton Tables in the subcritical range of pressures. A comparison of IFC data with our equation is given over a wider range of pressures for water in fig. 9. The only other cubic equation (actually a modified cubic that was not intended for use with water) close enough to the data to appear on this plot is
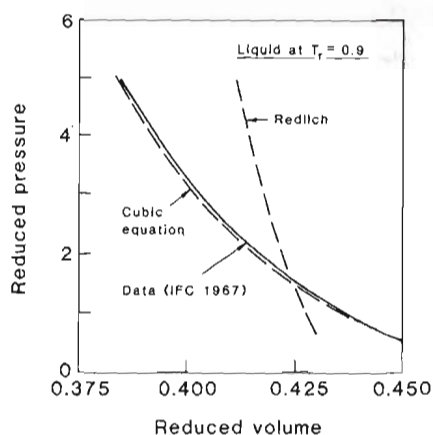


Fig. 9. Comparison of cubic equation, eq. (25), with IFC data [16] for liquid water at high pressures.

that of Redlich [22]. Fuller's [23] cubic equation – intended for water – predicts values outside the figure.

Another such comparison is presented for ethylene in fig. 10. The present cubic again outclasses the existing cubic equations and other "simple" equations. The key to this success is, of course, the fact that the coefficients are free from having to obey any predetermined dependence upon temperature.

We emphasize liquid properties because they are so hard to predict; however Murali [19] has shown that eq. (25) is extremely accurate in predicting superheated vapor properties.

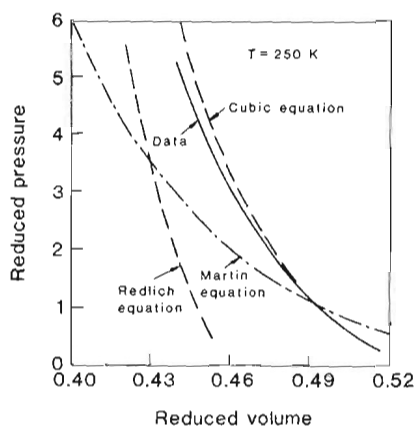But a most important use of the new equation of



Fig. 10. Comparison of cubic equation, eq. (25), to data for liquid ethylene at high pressures.

state is that of predicting properties in the metastable regimes. Fig. 11 compares the liquid spinodal of the cubic equation with the one predicted in ref. [3]. The agreement is very good except at such low temperatures and high liquid tensile stresses that both theories are being pushed to their limits of applicability.

The nucleation limits shown in fig. 11 are both obtained from eq. (15), using both $kT$ and $kT_c$: the use of $kT_c$ is far superior. The choice makes little difference in the positive pressure range, which is the only range in which experiments have ever been made for large $j$'s. At lower pressures the two diverge very strongly. Our recommendation to use $kT_c$ is largely based on the compelling evidence derived from the cubic equation. The value of $j$ used with the present cubic is $2 \times 10^{-5}$ instead of $10^{-5}$ (as recommended in ref. [3]) – a minor alteration. The replacement of $kT$ with $kT_c$ is the revolutionary issue here.

### 3.6. The prediction of surface tension

An acid test of any $p$–$v$–$T$ equation that purports to predict metastable and unstable properties is that is must correctly predict the temperature dependence of surface tension when it is used in van der Waals' surface tension eq. (22). The cubic equations for each isotherm
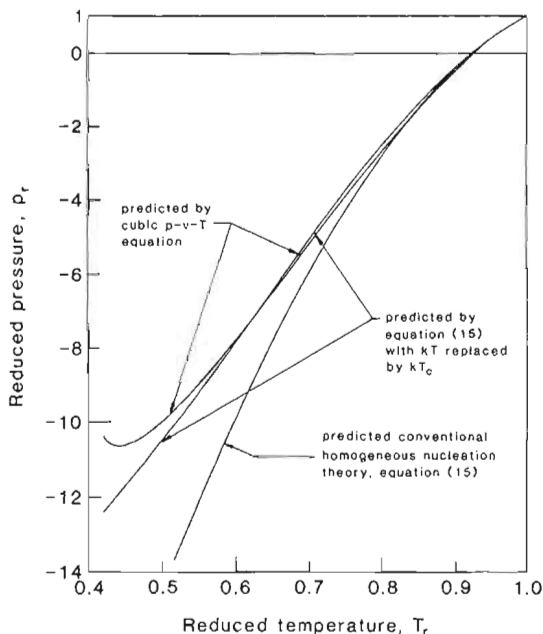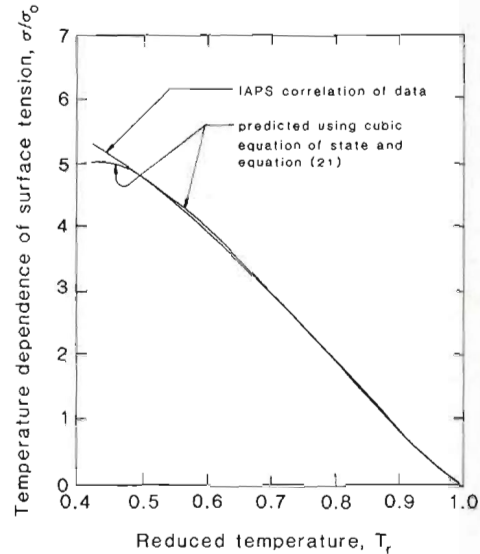


Fig. 12. Predicted and measured temperature dependence of surface tension.

have been subjected to this test * and the results are shown in fig. 12. Fig. 12 makes it quite clear that, except at the very lowest temperatures, the cubic equation passes this test with flying colors.

## 4. Depressurization of hot liquids

Consider a liquid in a container, suddenly depressurized from an initial point, ($p_i$, $T_i$), as shown in fig. 13. Such a system was studied both analytically and experimentally by Alamgir, Lienhard and Trela [24–26].

When the liquid is initially not too hot, or when the depressurization ends in nucleation well before the spinodal limit, the isentropic depressurization lies close to an isothermal path. Fig. 14 shows a typical pressure–time history for such a process from [25]. The sharpness with which the depressurization ends is very interesting. Experiments in ref. [26] showed that some nucleation occured on the pipe wall before the point at which depressurization abruptly reversed. Alamgir and Lienhard [25] therefore concluded that a real homogeneous nucleation limit was reached on the *two-dimensional* pipe wall.

Thus the homogeneous nucleation theory had to be



Fig. 11. Comparison of spinodal limit as predicted by homogeneous nucleation theory and by the general cubic equation.
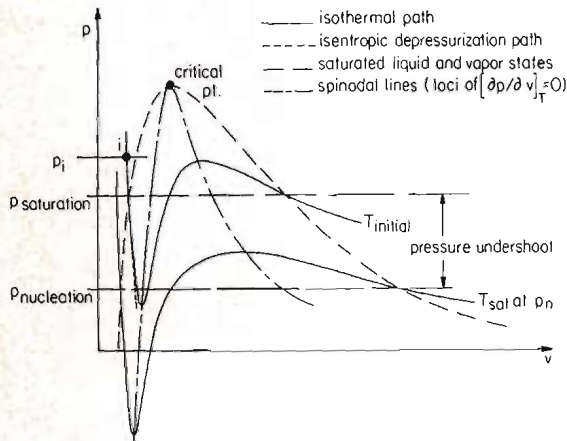
Fig. 13. Depressurization of a hot liquid.

reconstructed in a sort of "Flatland" form. Nucleation was taken to occur everywhere on the wall when the two-dimensional $J$ was equal to $10^{18}$ nucleation events/m$^2$ s. This translates to $j = 0.5661 \times 10^{-12}$ which is very close to $j$ for Skripov's pulse heating results.

The pressure undershoot, in this case, depends on the rate of depressurization, $\Sigma'$ atm/s (see fig. 14.) The reason is that a two-dimensional array of bubbles will have more time to grow and completely fill the wall if the rate is slower.

Alamgir and Lienhard [25] defined a "heterogeneity factor,"

$$\phi \equiv \frac{\text{actual potential barrier}}{\text{potential barrier for homogeneous nucleation}}$$
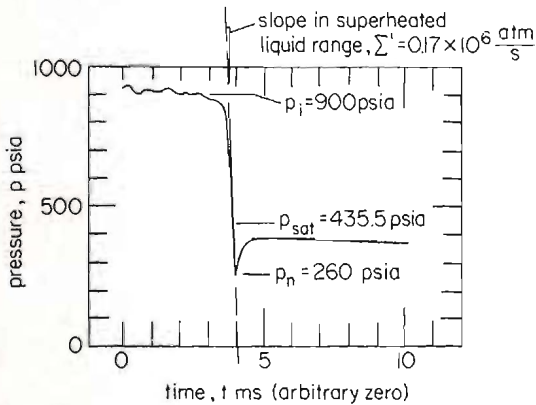


Fig. 14. A typical pressure–time history during depressurization in 453°F (233.9°C) liquid.

and an $\eta \equiv Gb/\phi$. Then they demonstrated that:

$$e^{-\eta\phi} - \sqrt{\pi\eta\phi}\ \text{erfc}\ \sqrt{\eta\phi}$$
$$= \frac{\Sigma'(1 - v_f/v_g)}{(N_A/v_f)^{2/3}(\text{collision rate})\sqrt{36kT\eta\sigma/\pi}}, \quad (26)$$

and used eq. (15) in the form applicable to real (not homogeneous) nucleation:

$$\eta = \frac{16\pi\sigma^3}{3kT(1 - v_f/v_g)^2(p_{sat} - p_n)^2}, \quad (15a)$$

to eliminate $\eta$ from eq. (26). They then used eq. (26) to calculate $\phi$ for observed nucleation events.

The resulting values of $\phi$ are correlated as a function of $\Sigma'$ and temperature in fig. 15. This correlation brings together the data of many investigators and it only breaks down when $\Sigma$ becomes so low that single isolated nucleation events can stop the depressurization. This occurs when $\Sigma'$ is less than 4000 atm/s.

The correlation shown in fig. 15 can be summarized in the form:

$$\phi(T_r, \Sigma') = 0.1058 T_r^{28.46}(1 + 14\Sigma'^{0.8}), \quad (27)$$

for

$$0.62 \leq T_r \leq 0.935, \quad 0.004 \leq \Sigma' \leq 1.8\ \text{Matm/s}.$$

which correlates all available blowdown data with a 10.4% rms error.

The data in fig. 15 imply that $j$ is $0.5661 \times 10^{-12}$. This gives Gb = 28.2. By substituting Gb/$\phi$ for $\eta$ in eq. (15a) and using eq. (27), we recast the undershoot prediction in dimensional form:

$$p_{sat}(T_i) - p_{nucleation} = 0.252 \frac{\sigma^{3/2}T_r^{13.73}(1 + 14\Sigma'^{0.80})^{0.5}}{\sqrt{kT_c(1 - v_f/v_g)}}. \quad (28)$$

For the reader's convenience, this pressure undershoot is displayed in dimensional form for water, as a function of $\Sigma'$ and the initial saturation temperature, $T_i$, in fig. 16.

### 4.1. The damage-doing potential of a sudden depressurization

A most important practical problem is that of answering the question: "A large pipe carrying nearly-saturated water at high pressure is suddenly ruptured. How much damage can each pound of water do to the
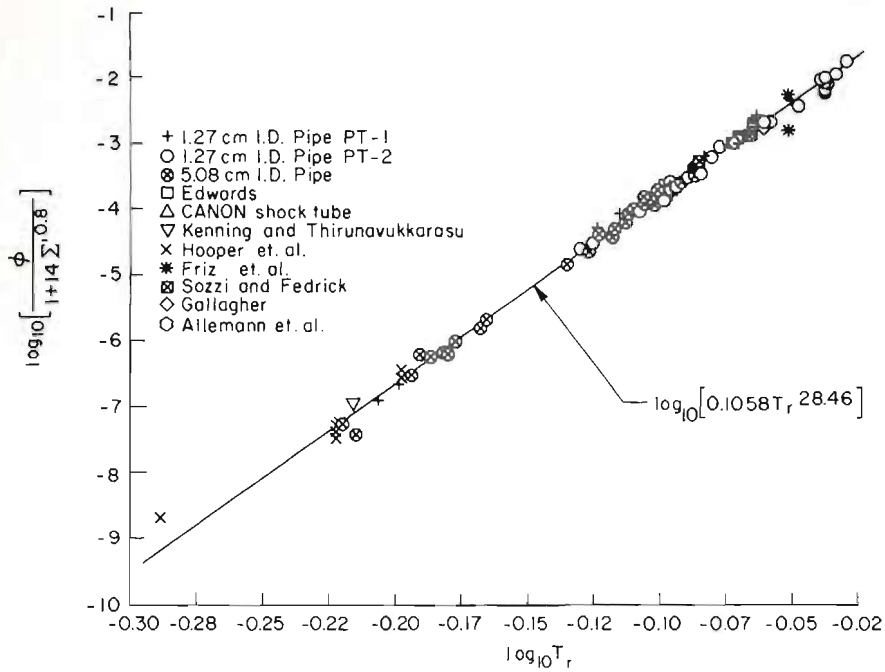
a) The function, $f_1(T_r) = \phi / f_2(\Sigma')$
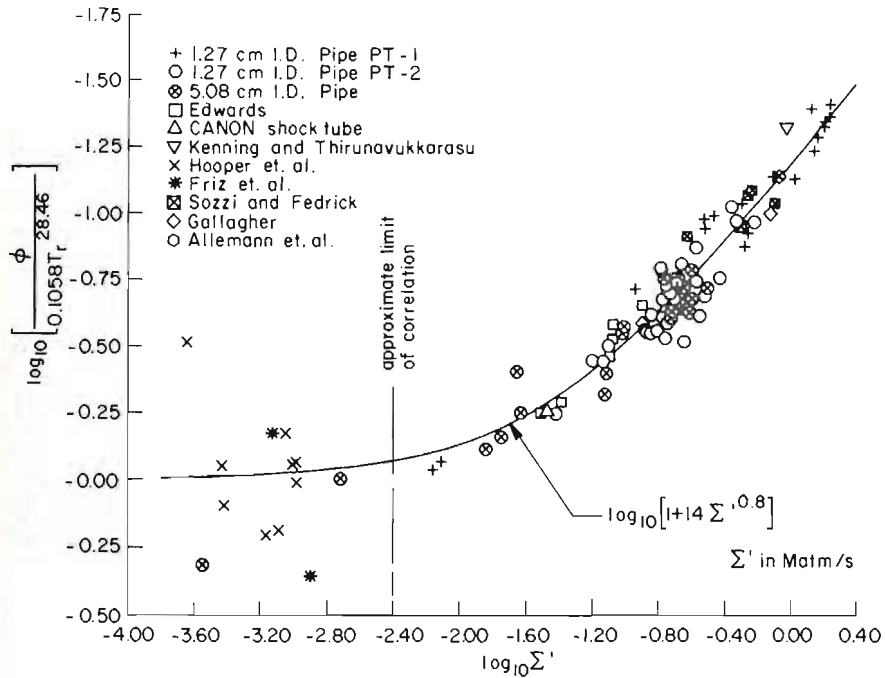


b) The function, $f_2(\Sigma') = \phi / f_1(T_r)$

Fig. 15. Correlation of $\phi$ as a function of liquid temperature and the rate of depressurization.
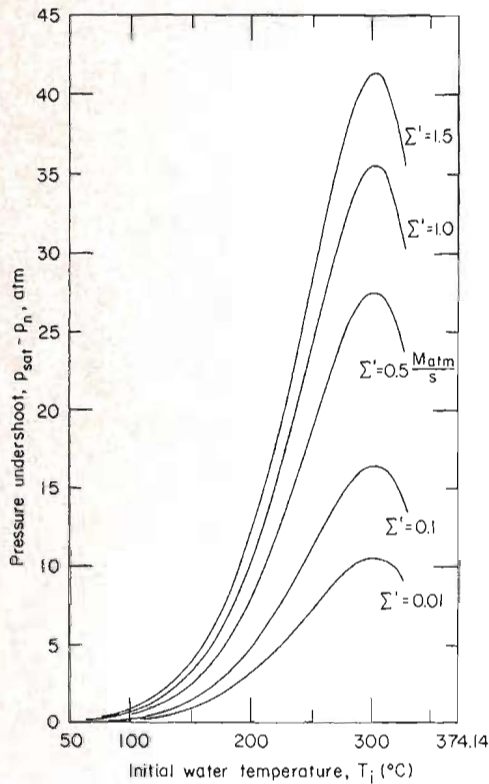
Fig. 16. Prediction of pressure undershoot applied to water.

A description of the exact calculation, and the evaluation of $\Delta a$ for van der Waals fluids at their spinodal lines are given in ref. [4]. We have also computed availabilities of superheated water for EPRI using Karimi's fundamental equation. One of these calculations involved challenging the often-used assumption that isentropic depressurizations can be treated as isothermal. Fig. 17 shows what the left-hand region of fig. 1 or 13 would look like plotted to scale. Notice that at $T_r = 0.8855$ (or $T = 300°C$) the assumption is not bad as long as the pressure stays positive; but at $T_r = 0.9627$ (350°C) it breaks down much more quickly.

This information is shown in another way in fig. 18 which shows how the relation between $p$ and $T$ changes along isentropic paths, starting from various initial saturation temperatures.

Fig. 19 shows how the availability of water above the normal boiling point, varies with the temperature at which it first crosses the saturated liquid line. As $p$ decrease, the availability diminishes, but the reduction is too little to improve safety noticeably. A *very* rapid depressurization of 1.5 Matm/s brings water to nucleation at a point whose availability almost matches the saturation point from which depressurization began. The point where nucleation occurs in fig. 19 is obtained with the help of eq. (28). It is sobering that $\Delta a$ is on the

system in the resulting thermohydraulic explosion?" Two thermodynamic issues lurk in this important safety-related question. The first – that of saying how far below its saturation pressure the water must fall before an explosion is initiated – is answered by eq. (28).

The second issue is that of determining the thermodynamic availability of the liquid at this limit. The availability of a liquid with respect to its surroundings specifies the maximum "useful" work – actually damage in this case – that it can deliver to these surroundings. The latter issue requires a knowledge of the thermodynamic properties of metastable liquids.

The isobaric availability of a slightly superheated liquid with respect to its saturation state is (recall eq. (14)):

$$\Delta a = \int_{T_{sat}}^{T_{sup}} c_p \, dT - T_{sat} \int_{T_{sat}}^{T_{sup}} (c_p/T) dT. \tag{29}$$

By assuming $c_p$ is constant – which is certainly untrue at high superheats – we obtain as a limit for low superheat (see ref. [27].)

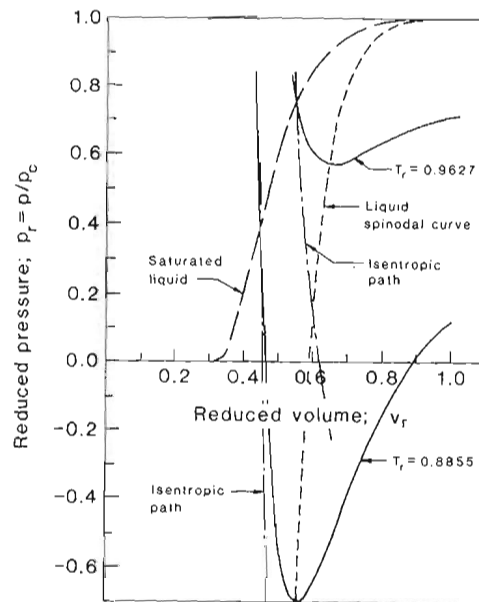$$\Delta a = c_p \Delta T^2 / 2T_{sat}. \tag{30}$$



Fig. 17. Comparison between isentropic and isothermal depressurizations in water.
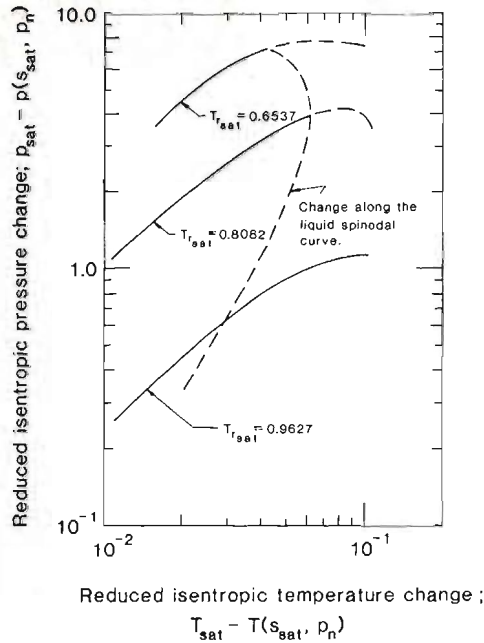
Fig. 18. The relation between pressure and temperature during three isentropic processes in water.
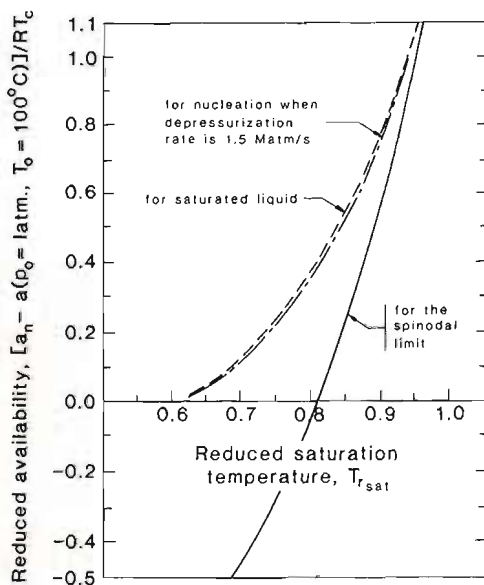


Fig. 19. Availability of water, when it nucleates, in comparison with saturated water at one atmosphere. The independent variable is the reduced temperature at which the liquid becomes saturated during depressurization.

order of $RT_c$, or about $10^5$ ft-lb$_f$/lb$_m$ for water. Thermohydraulic explosions can do a lot of damage.

## 5. Summary

This review clearly reflects the ongoing interests of its authors, and new results are currently being developed. New papers still under review at this writing include the development of corresponding correlations of saturated and metastable $p-v-T$ properties [28], further description of the cubic equation development, and the prediction of surface tension from cubic equations [29]. The important points of the present discussion are:

(1) There is a real need to be able to predict spinodal lines, homogeneous nucleation, and properties of superheated liquids.

(2) These issues present an inherent inter-relation of purposes:
  - A knowledge of metastable and unstable $p-v-T$ behavior facilitates the extrapolation of single measurements of $\sigma$ over the full range of temperatures. By the same token, a knowledge of $\sigma(T)$ provides an important check on any equation of state.
  - The ability to predict homogeneous nucleation and the ability to predict the liquid spinodal are equivalent.
  - Thus knowledge of the $p-v-T$ surface includes knowledge of the liquid spinodal and the limit of homogeneous nucleation as well.

(3) Eq. (15) predicts homogeneous nucleation in a variety of practical situations:
  - By replacing the left side with the $-\ln j$ appropriate to a real situation, one can use it to handle real situations.
  - If $v_f$, $v_g$ and $\sigma$ are not available for eq. (15), correlations (17) and (18) can be used with good accuracy.

(4) The vapor spinodal is unrelated to the limit of homogeneous nucleation of liquid droplets.

(5) Strong evidence suggests that homogeneous nucleation theories should be based on the characteristic energy, $kT_c$, instead of $kT$.

(6) Metastable $p-v-T$ data can be accurately predicted by fitting a general cubic equation to the known saturation points, a known saturated liquid compressibility, a third stable equilibrium point and the Gibbs–Maxwell condition.

(7) When more than just $p-v-T$ data are needed, Karimi's method can be used to develop a funda-

mental equation, but it should be altered to use a more realistic reference function.

(8) Karimi's fundamental equation provides the best information for metastable water, to date.

(9) Eq. (28) predicts the pressure undershoot in the rapid depressurization of hot water. It reflects the fact that sufficiently rapid depressurizations reach a true (two-dimensional) homogeneous nucleation limit.

## Nomenclature

| | | |
|---|---|---|
| $a$ | = | availability function, or |
| $a, b$ | = | van der Waals constants (eq. (3)). (also used in other equations of state as undetermined constants.) |
| $c, d$ | = | undetermined constants (which could be complex conjugates) |
| $c_p, c_p^0$ | = | specific heat at constant pressure, low pressure $c_p$ |
| $g$ | = | specific Gibbs function, or function of $\omega$ defined in fig. 3 |
| Gb | = | Gibbs number (see eq. (9)) |
| $h$ | = | specific enthalpy |
| $j, J$ | = | nucleation probability (see eq. (10)); $j$ expressed as a rate per unit volume |
| $k$ | = | Boltzmann's constant |
| $m, n$ | = | undetermined constants |
| $p$ | = | pressure |
| $Q$ | = | residual correction function for a fundamental equation |
| $R$ | = | ideal gas constant |
| $R_0$ | = | critical radius of nucleation (see eq. (8)) |
| $s$ | = | specific entropy |
| $T$ | = | temperature |
| $u$ | = | specific internal thermal energy |
| $v$ | = | specific volume |
| $v, v_f, v_g$ | = | saturated liquid and vapor volume. (at the saturated spinodal condition in eq. (15)) |
| $v_m$ | = | $v$ at the root of a cubic $p-v-T$ equation between $v_f$ and $v_g$ |
| Wk$_{crit}$ | = | potential barrier to nucleation (see eq. (7)) |
| $Z_c$ | = | critical compressibility, $p_c v_c / R T_c$ |
| $\alpha, \alpha_R$ | = | $(\alpha_R + \lambda)/(1 - \lambda)$; the Riedel factor |
| $\eta$ | = | Gb/$\phi$ |
| $\lambda$ | = | nondimensionalizing factor, defined in ref. [10]. Also an undetermined constant in eq. (23). |
| $\sigma, \sigma_0$ | = | surface tension, an undetermined reference value of $\sigma$ |

| | | |
|---|---|---|
| $\phi$ | = | ratio of actual to ideal potential barrier to nucleation |
| $\psi$ | = | Helmholtz function |
| $\omega$ | = | the Pitzer factor, $-1 - \log_{10}[p_{r,sat}(T_r = 0.7)]$ |

*General superscripts and subscripts*

| | | |
|---|---|---|
| $'$ | = | denotes a dummy variable of integration, or the dimensional forms of $a$, $b$, $c$ and $d$ |
| c | = | a property at the critical point |
| f, g | = | saturated liquid or vapor properties |
| fsp, gsp | = | identify liquid and vapor spinodals in fig. 6 |
| h.n. | = | a homogeneous nucleation limit |
| r | = | a "reduced" property (e.g. $X_r \equiv X/X_c$) |
| ref | = | a reference state |
| sat | = | a property at a saturation condition |
| sp | = | a property at a spinodal point |

## References

[1] A. Karimi and J.H. Lienhard, Toward a fundamental equation for water in the metastable states, High Temp. – High Press. 11 (1979) 511–517.

[2] A. Karimi and J.H. Lienhard, A fundamental equation representing water in the stable, metastable and unstable states, EPRI Report NP-3328 (Dec. 1983).

[3] A. Karimi and J.H. Lienhard, Homogeneous nucleation and the spinodal line, J. Heat Transf. 102 (1980) 457–460.

[4] N. Shamsundar and J.H. Lienhard, Properties of the saturated and metastable van der Waals fluid, Can. J. Chem. Engr. 61 (1983) 876–880.

[5] J.H. Lienhard, Corresponding states correlations of the spinodal and homogeneous nucleation limits, J. Heat Transf. 104 (1982) 379–881.

[6] Md. Alamgir and J.H. Lienhard, Correlation of pressure undershoot during hot water depressurization, J. Heat Transf. 103 (1981) 52–55.

[7] Md. Alamgir, C.Y. Kan and J.H. Lienhard, An experimental study of the rapid depressurization of hot water, J. Heat Transf. 102 (1980) 433–438.

[8] L. Riedel, Eine neue universelle Dampfdruckformel, Chemie-Ing. Technik 25 (1954) 83.

[9] K.S. Pitzer, D.Z. Lippman, R.F. Curl, C.M. Huggins and D.E. Peterson, J. Am. Chem. Soc. 77 (1955) 3433.

[10] A. Sharan, R. Kaul and J.H. Lienhard, A corresponding states correlation for the peak pool boiling heat flux, J. Heat Transf. 107 (1985) 392–397.

[11] V.P. Skripov, Metastable Liquids (1970), English translation (John Wiley and Sons, New York, 1974).

[12] V.P. Skripov, E.N. Sinitsin, P.A. Pavlov, G.V. Ermakov, G.N. Muratov, N.V. Bulanov and V.G. Baidakov, Thermophysical Properties of Liquids in the Metastable State (Atomizdat, USSR, 1980).

[13] C.T. Avedisian, The homogeneous nucleation limits of liquids, J. Phys. Chem. Ref. Data, in press.

[14] J.H. Lienhard, Correlation for the limiting liquid superheat, Chem. Engr. Sci. 31 (1976) 847–849; see also: J.H. Lienhard and A. Karimi, Homogeneous nucleation and the spinodal line, J. Heat Transf. 103 (1981) 61–64.

[15] J.H. Keenan, F.G. Keyes, P.G. Hill and J.G. Moore, Steam Tables (John Wiley and Sons, New York, 1969).

[16] Steam Tables, 4th Ed. (American Society of Mechanical Engineers, New York, 1979).

[17] J.D. Van der Waals, Thermodynamische Theorie der Kapillarität unter Voraussetzung stetiger Dichteänderung. Zeit. Phys. Chem. 13 (1894) 657–725.

[18] L. Haar, J.S. Gallagher, G.S. Kell, Thermodynamic properties for fluid water, in: Water and Steam, Eds. J. Straub and K. Scheffler (Pergamon Press, New York, 1980) pp. 69–82.

[19] C.S. Murali, Improved cubic equations of state for polar and non-polar fluids, MSME thesis, Dept. of Mech. Engr., Univ. of Houston (1983).

[20] N.B. Vargaftik, Tables of Thermophysical Properties of Liquids and Gases, 2nd Ed. (Hemisphere Publishing Co., Washington, 1975).

[21] C.T. Ewing, J.P. Stone, J.R. Spann and R.R. Miller, High temperature properties of sodium, J. Chem. Engr. Data 1 (1966) 468.

[22] O. Redlich, On the three-parameter representation of equation of state, I.E.C. Fundamentals 14 (1975) 257.

[23] G.G. Fuller, A Modified Redlich–Kwong–Soave equation capable of representing the liquid state, I.E.C. Fundamentals 15 (1976) 254.

[24] J.H. Lienhard, Md. Alamgir and M. Trela, Early response of hot water to sudden release from high pressure, J. Heat Transf. 100 (1978) 473–479.

[25] Md. Alamgir and J.H. Lienhard, Correlation of pressure undershoot during hot water depressurization, J. Heat Transf. 103 (1981) 52–55.

[26] Md. Alamgir, C.Y. Kan and J.H. Lienhard, An experimental study of the rapid depressurization of hot water, J. Heat Transf. 102 (1980) 433–438.

[27] J.H. Lienhard, Some generalizations on the stability of liquid–gas–vapor systems, Int. J. Heat Mass Transf. 7 (1964) 813.

[28] W-g. Dong and J.H. Lienhard, Corresponding states correlation of saturated and metastable properties, Canadian J. Chem. Engrg. 64 (1986) 158–161.

[29] P.O. Biney, W-g. Dong and J.H. Lienhard, Use of a cubic equation to predict surface tension and spinodal limits, J. Heat Transf. 108 (1986) 405–410.